RSC Advances

Few-atomic-layer boron nitride sheets synthesized in solid thermal waves

Journal:	*RSC Advances*
Manuscript ID:	RA-ART-09-2014-010907.R2
Article Type:	Paper
Date Submitted by the Author:	18-Dec-2014

Complete List of Authors:	Nersisyan, Hayk; Chunnam National University, Lee, Tae-Hyuk; Chungnam National University, Lee, Kap-Ho; Chunnam National University, Lee, Jin-Seok; Korea Institute of Energy Research, Ahn, Young-Soo; Korea Institute of Energy Research, Lee, Jong-Hyeon; Chungnam National Univ., Metallurgical Engineering; Chungnam National Univ., Green Energy Technology

Graphical abstract

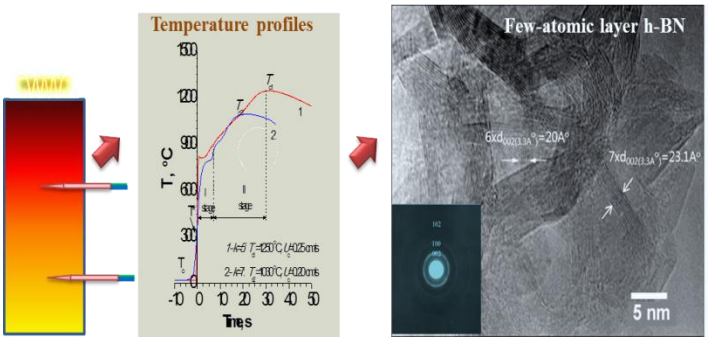

A few-atomic-layer hexagonal boron nitride (h-BN) sheets were synthesized in a solid thermal wave implemented in a B_2O_3+(3+0.5*k*)Mg+*k*NH_4Cl mixture.

Journal Name

RSCPublishing

ARTICLE

Few-atomic-layer boron nitride nanosheets synthesized in solid thermal waves

Hayk H. Nersisyan[a,c], Tae-Hyuk Lee[a], Kap-Ho Lee[a], Young-Soo An[d], Jin-Seok Lee[d], and Jong-Hyeon Lee[a,b,c*]

Cite this: DOI: 10.1039/xoxxoooooox

Received ooth January 2012,
Accepted ooth January 2012

DOI: 10.1039/xoxxoooooox

www.rsc.org/

In this study, we demonstrate the synthesis of few-atomic-layer hexagonal boron nitride (h-BN) sheets in a solid thermal wave implemented in a B_2O_3+(3+0.5*k*)Mg+*k*NH_4Cl exothermic mixture (here, *k* is the mole number of NH_4Cl). The maximum synthesis temperature, developed using a thermal wave, was between 1030 and 1250 ^oC as *k* was changed from 5 to 7 moles. The phase content, morphology, and optical properties of the products were characterized. It is shown that BN sheets synthesized at the given *k* were 1.5-3 nm thick and had a hexagonal structure. The number of atomic layers in one sheet ranged from 5 to 10; the lateral dimension of individual sheets ranged from 50 to 1000 nm. The developed method allowed the synthesis of a large amount of uniform and high quality BN nanosheets (tens of grams in laboratory-scale experiment); this method will reduce the overall production cost.

1. Introduction

Atomically thin hexagonal boron nitride (h-BN), as a graphene analogue, is a wide-band gap insulator with a lattice constant similar to that of graphene; it has very high mechanical strength and good thermal conductivity because of the strong B-N covalent sp^2 bonds in its plane, as well as excellent chemical and thermal stability.[1-5] As a result, h-BN has a wide range of applications, such as deep ultraviolet light emitters, transparent membranes, protective coatings, and dielectric layers.[1,2,6] In addition, h-BN layers have great potential for use when combined with graphene as constituent layers to create a new class of functional multilayer heterostructures and devices.[7-10] Previous studies have shown that h-BN can be used as a substrate material for high-performance graphene electronics because it has an atomically smooth surface that is relatively free of dangling bonds and trapped charges.[8,9] Recently, h-BN has been used as a barrier layer between two graphene layers to construct vertical tunnelling transistors.[10,11] Similar to the case of graphene, controlled synthesis of large-area high-quality h-BN with different numbers of layers is essential for both fundamental studies and technological applications.

Currently, several methods have been developed to prepare atomically thin h-BN including micromechanical cleavage,[10-14] liquid-phase exfoliation,[15] chemical vapour deposition (CVD)[4,9,16-26], and surface segregation[27]. Among these methods, CVD has shown promise for the preparation of large-area h-BN films; such films opens up possibilities for the use of h-BN in large-scale electronics. Large-area inhomogeneous few-layer and multilayer h-BN films have been prepared on polycrystalline Cu or Ni using ambient pressure CVD (APCVD) with ammonia borane (H_3BNH_3, also called borazane) or borazine ($H_3B_3N_3$) as precursors.[4,9,16,25,26] Monolayer h-BN was first synthesized in ultrahigh vacuum (UHV) systems mostly using borazine as a precursor and single-crystal metals such as Pt(111), Rh(111), Ru(0001), Cu(111), and Ni(111) as substrates.[7-20,22,23] Recently, Kim et al.[20] realized the growth of monolayer h-BN on Cu foil using low-pressure CVD (LPCVD) with borazane as the precursor. Ismach et al. showed controlled synthesis of h-BN with number of layers from 1-5 to ~100 on Ni foil using LPCVD with diborane and ammonia as precursors. [23] Gao et al.[24] reported an ambient pressure/CVD method for few-layer BN synthesis from borazane using PT catalyst. However, using CVD, it is still very challenging to precisely control the number of layers of h-BN. M. Xu et al. [27] reported that few-layer hexagonal boron nitride (h-BN) nanosheets can be produced by using a surface segregation method: vacuum thermal treatment of iron–chromium–nickel (Fe–Cr–Ni) alloys doped with boron (B) and nitrogen (N). The formation of h-BN sheets is via an intermediate boron–nitrogen buffer layer. The experimental results suggest that surface segregation of boron and nitrogen from a solid source is an alternative approach to tailoring the synthesis of h-BN sheets for use in potential applications such as graphene electronics. X. Wang et al.[28] reported a "chemical blowing" approach relies on making large bubbles with atomically thin B-N-H polymer walls using H_2 gas produced from an ammonia borane compound precursor. However, because all of these methods use specific reaction systems and expensive and harmful raw materials, they may not support the large-scale production of h-BN at low cost.

The preparation of BN by solution combustion method combined with a high-temperature nitridation process was

reported by Zhao et al.[29] In this process, the authors at first prepared a water solution containing H_3BO_3, NaN_3, NH_4Cl, and $(NH_2)_2CO$, which was then dried in air and heated in a muffle furnace at 600 °C for combustion. Then, the resultant product was washed with de-ionized water, dried in vacuum, and annealed between 1000 °C and 1400 °C in a nitrogen atmosphere to obtain BN nanoplates having diameters in a range of 300–500 nm and thicknesses below 30 nm. However, this approach is technologically ineffective due to a number of time-consuming heating steps, is thermodynamically unfavourable, and contains NaN_3, which is a fire and explosion hazard.

Here, for the first time, we report an alternative facile solid combustion route (also called the solid flame process) for the synthesis of few-atomic-layer h-BN sheets in a solid thermal wave of B_2O_3+(3+0.5*k*)Mg+*k*NH_4Cl exothermic mixture. Two main steps can be distinguished in this method: the combustion of a solid mixture in a nitrogen atmosphere followed by the acid leaching of the combustion product. Few-layer BN nanosheets produced using the designed method have great promise in the further preparation of ultra-thin films with large surface-to-volume ratio. The developed method allows the synthesis of a large quantity of BN nanosheets (tens of grams in laboratory scale experiment), which may essentially reduce process pollution and decrease the production cost. Moreover, we have demonstrated that the as-synthesized BN nanosheets are very uniform, with high quality and a smooth surface.

2. Results and discussion

For the synthesis of h-BN few-atomic-layer sheets, an exothermic mixture of B_2O_3+(3+0.5*k*)Mg+*k*NH_4Cl composition (here, *k* is mole number of NH_4Cl) was prepared in the form of a cylindrical pellet and combusted in a nitrogen atmosphere. Preliminary experiments revealed that the reduction of B_2O_3 by Mg in the presence of NH_4Cl may result in h-BN thin sheets and that the thickness of these sheets depends on the concentration of NH_4Cl. To decrease the thermal wave temperature to a value below 1300 °C and to produce few-atomic-layer h-BN, the optimum concentration of NH_4Cl is between 5 and 7 mol.

The characteristics of the initial reaction mixture (for *k*=5) were analysed using differential scanning calorimetry and thermogravimetric analysis (DSC-TGA); results are shown in Fig. 1.

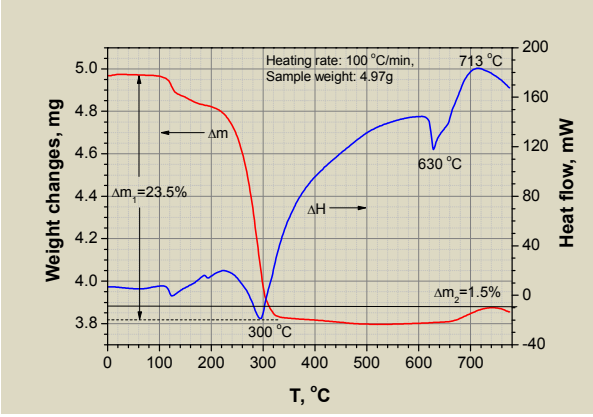

Fig. 1. TGA-DSC analysis of B_2O_3+ 5.5Mg+5NH_4Cl mixture.

Approximately 4.97 mg of the mixture was heated at a rate of 100°C/min in a platinum crucible under a flow of nitrogen (80 sccm). A high heating rate was chosen in order to bring the heating process closer to the combustion regime. The analysis revealed two endothermic peaks on the DSC curve, at 300 °C and 630 °C. The endothermic peak at 300 °C might originate from the thermal decomposition of NH_4Cl, whereas the peak at 630 °C originates from Mg melting. The continuous increase in the heat flow curve in the temperature range of 300-630 °C can be explained as resulting from a partial reaction between Mg and NH_4Cl. The small exothermic peak around 713 °C is consistent with the exothermic reduction of B_2O_3 by Mg. The corresponding TGA curve revealed a 23.5 wt% weight loss in the temperature range of 100 to 350 °C due to the partial decomposition of NH_4Cl. Then, beyond this temperature range, the total weight of the sample remains constant until 650 °C. Above 650 °C, the weight was found to slightly increase (~1.5 wt %), which may be associated with the partial formation of Mg_3B_2 phase, which formation is predicted by thermochemical analysis (Fig. 1S).

Figure 2 shows typical temperature–time profiles for the B_2O_3+(3+0.5*k*)+ *k*NH_4Cl mixture at *k*=5 and 7. These profiles are started by a thermal layer (left side of ordinate) with an exponentially growing temperature in the combustion zone (right side of ordinate). The starting (ignition) temperature for the combustion process is 300 °C, as denoted by T*; this temperature was determined from the DSC curve. Conditionally, the reaction zone can be split into two stages, I and II. Stage I involves the chlorination of magnesium, which occurs in a temperature range of 300-800 °C, whereas stage II is responsible for the reduction-nitridation processes of boron. The quasi-isothermal region between these two stages most likely is associated with the melting of $MgCl_2$ ($T_{melt.}$=714 °C). The maximum combustion temperatures (T_c), estimated from the temperature slopes, are

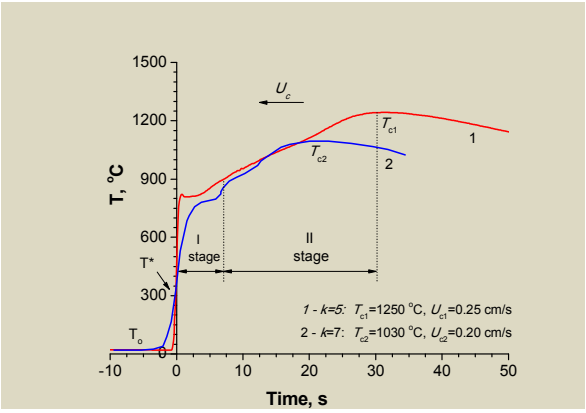

Fig. 2. Temperature-time profiles in the combustion wave of B_2O_3+(3+0.5*k*)Mg+*k*NH_4Cl system.

1250 °C and 1030 °C for *k*=5 and 7, respectively. The combustion velocity (U_{c1}) of the reaction mixture, for k=5, was found to be 0.25 cm/s (Fig. 2). When the amount of NH_4Cl is increased to *k*=7 mol, the combustion velocity (U_{c2}) drops to 0.2 cm/s. With a higher concentrations of NH_4Cl (k>7) the combustion of the initial mixture failed. In both cases (*k*=5 and 7) the appearance of the reaction sample was found to change from the grey to white, as shown in Fig 3ab. This indirectly indicates that BN phase was successfully formed during the combustion process. Therefore, after acid leaching and water

purification of the combustion product, a white powder with good lubrication properties was obtained (Fig. 3c).

The hexagonal crystal structure of the BN powders was further confirmed by X-ray diffraction measurement (XRD) of the acid leached samples (Fig. 4). The h-BN (002) and (100) peaks at around 26.7 and 41.8° were identified. The estimation of the interlayer spacing according to Bragg's law is 0.33 nm, which is consistent with the value from the TEM measurement. It is also clear that the broadening of the XRD peak indicates that the diameter of the BN particles is small.

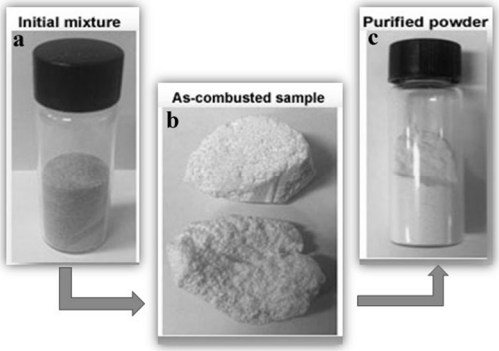

Fig. 3. Images of reaction species: a - initial mixture; b – large pieces of as-combusted sample; c - acid leached powder

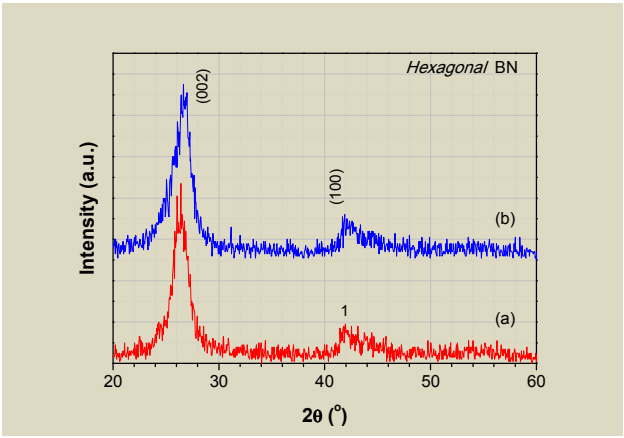

Fig. 4. XRD patterns of purified h-BN samples versus *k*: (a) *k*=5; (b) *k*=7.

Transmission electron microscopy (TEM) with a JEOL JEM 1400 was used to characterize the structure and thickness of the *h*-BN particles; the results are shown in Fig. 5.

The top images show the morphology of the BN particles synthesized at *k*=5 and 7 (Fig. 5a and b). The TEM images of the BN surface revealed structures with bifurcating curved fringes. The lateral dimensions of the as-synthesized nanosheets ranged from 50 to 1000 nm, as estimated from the high resolution FE-SEM (Fig. 3S, ESI). In Fig. 5c, parallel line features can be observed along the edge of the sheet under high magnification. The number of layers in one sheet is from 5 to 10, as estimated from Fig. 5c. This allows not only the counting of the number of layers of the nanosheets but also the measurement of the interlayer distance, which is around 0.33 nm, consistent with the reported value for h-BN structure.[30]

SAED patterns of the BN nanosheets shown in the inset of Fig. 5c suggest that all rings on the diffraction patterns belong to the hexagonal BN phase, that the as-synthesized nanosheets have a good crystalline nature, and that the lattice parameters are a=2.5044A°; c=6.6562A°.

Raman and FTIR spectroscopy, in which phonons are excited by inelastic scattering of light and light absorption, respectively, are convenient tools to investigate the phonon features and phase purity of the samples. Fig. 6 shows the high-frequency Raman spectrum of boron nanosheets. According to the literature, only two characteristic Raman active B-N vibrational modes – the in-phase E_{2g} mode (50 cm^{-1}) and the counter-phase E_{2g} mode (1367 cm^{-1}) are present for h-BN.[31] As shown in Fig. 6, a dominant sharp peak at 1366.4 was found, which corresponds to the counter-phase BN vibrational mode (E_{2g}) within the BN sheets. The peak of the as-prepared BN nanosheets is slightly down-shifted (about 0.6 cm^{-1}) compared with the well-known value of nanosheets (1367 cm^{-1}) of bulky h-BN.

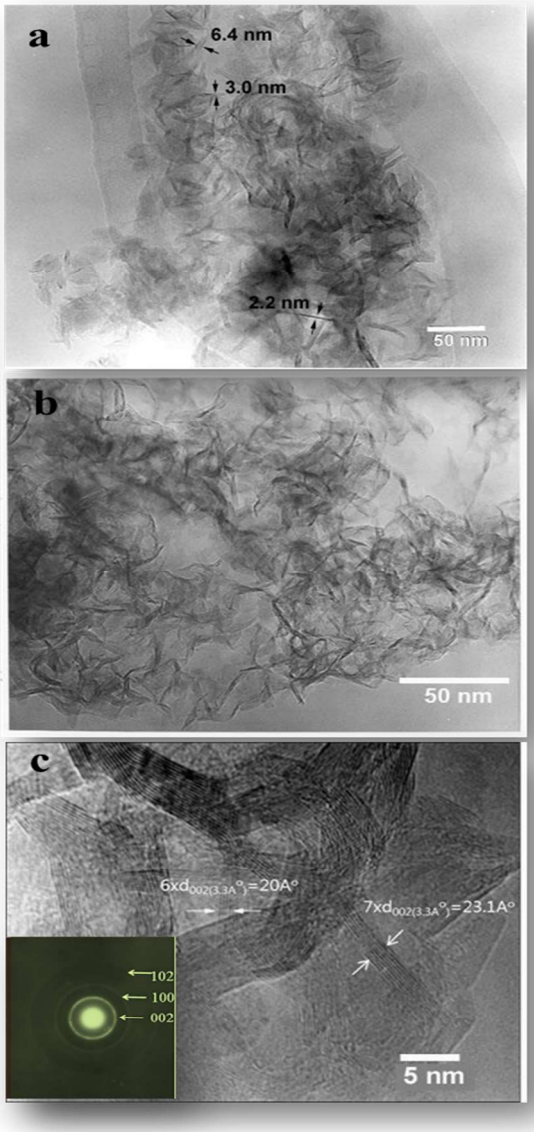

Fig. 5. TEM and HR-TEM images and corresponding SAED patterns (the inset) of purified BN samples: a - *k*=5; b and c- *k*=7.

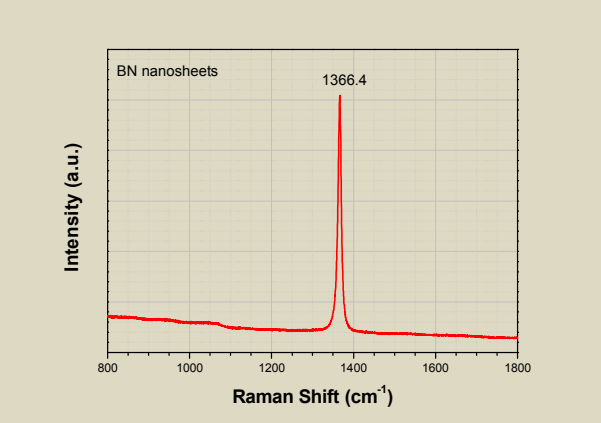

Fig. 6. Raman spectrum of h-BN nanosheets prepared at *k*=5.

The FWHM of the peak is ~15 cm^{-1}, which is wider than that observed for h-BN single crystals obtained by high-pressure and high-temperature synthesis (9.1 cm-1)[32], and is close to that observed for pure BNNTs (13 cm^{-1})[33] and BN nanosheets prepared by microwave plasma chemical vapour deposition method (MPCVD).[34]

More information on the lattice vibrations and composition can be gained through FTIR characterization. Fig. 7 shows the typical FTIR spectrum of the products, in which two strong characteristic peaks positioned at 1379 and 812 cm^{-1} are observed. The broad peak at 1379 cm^{-1} is ascribed to E_{1u} (B–N stretching vibration mode perpendicular to the c-axis) modes of h-BN, while the absorption band of the sharper, weaker peak at 811 cm^{-1} is attributed to A_{2u} (B–N–B bending vibration mode parallel to the c-axis)[35]. No obvious absorption peaks associated with the starting materials and carbon or oxygen are observed, which indicates the high purity of h-BN nanosheets.

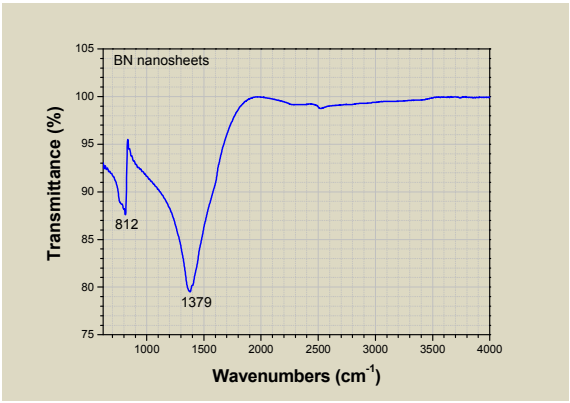

Fig. 7. FTIR spectrum of h-BN nanosheets prepared at *k*=5.

The formation of h-BN nanosheets in solid combustion wave of B_2O_3+(3+0.5*k*)Mg+*k*NH_4Cl mixture (*k*=5-7) is a complex physical-chemical process consisting of a large number of elementary reactions. Among them, at least three basic reactions can be distinguished and formulated as follows:

$2NH_4Cl + Mg \rightarrow MgCl_2 + 2N_2 + H_2$ (1)

$B_2O_3 + 3Mg \rightarrow 3MgO + 2B$ (2)

$B+0.5\ N_2 \rightarrow BN$ (3)

Reaction (1) is a low-temperature reaction and occurs in the initial stage of the combustion process, right after the ignition of the reaction mixture. Then, the reduction of B_2O_3 by magnesium (2) and the nitridation of the reduced boron (3) follows. Reaction (1) has several key functions during the formation of BN nanosheets. First, the decomposition of NH_4Cl results in a high concentration of nitrogen gas inside the reaction pellet; the nitridation of boron particles becomes significantly activated. Meanwhile, the as-formed BN nanosheets are immediately coated by a molten layer of $MgCl_2$ and the grain growth process is stopped. Therefore, after acid washing and water purification of the reaction products, few-layer BN nanosheets were successfully obtained.

3. Experimental

Powders of B_2O_3 (95% pure, particle size 50-300 μm, Junsei Chemical Co., Ltd., Japan) and Mg (99% pure, particle size: 50-200 μm, Samchun Chemicals and Metals Co., Ltd., Korea) were used as the starting materials for the synthesis of BN nanosheets. NH_4Cl (99% pure, Samchun Chemicals and Metals Co., Ltd., Korea) was used as a solid source of nitrogen to increase the concentration of nitrogen inside the reaction pellet and to control the combustion temperature. For these purposes, a mixture of B_2O_3+(3+0.5*k*)Mg +*k*NH_4Cl composition (*k* is mol number of NH_4Cl) was used in the combustion experiment: (*k*) added to the main mixture was controlled so as to be in the range of 5– 7 mol.

The experimental set-up used for the synthesis of BN nanosheets is shown in Fig. 8. The set-up consists of a nitrogen ballon (1) connected to a high-pressure combustion chamber (2) and a data logger (3) for recording the signals from the thermocouples.

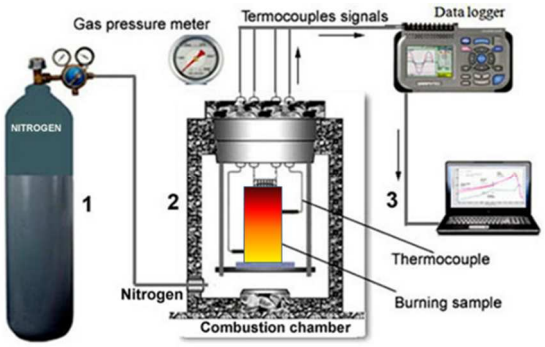

Fig. 8. Experimental set-up used for synthesis of BN nanosheets.

In a typical experiment, a reaction mixture of about 100 g of raw materials prepared by hand mixing in a ceramic mortar was hand-compacted into a paper cup (diameter: 4.0 cm; height: 8-9 cm). During compaction, two Λ-shaped tungsten-rhenium thermocouples (WR-26/WR-5), 100 μm in diameter, were put into the centre of the sample. Individual thermocouples were coated with a thin layer of Al_2O_3 (~5–10 μm) to increase their resistance to oxidation and to avoid a possible interaction between the thermocouples and the powder bed at elevated temperatures. Approximately 2–3 g of Ti + 0.9C (black soot) +

$0.1[(C_2F_4)_n]$ was placed on top of the reaction sample as an ignition agent. The cup containing the reaction mixture and the thermocouples was subsequently placed under a nickel/chromium coil in the combustion chamber. The chamber was then filled with 2.5 MPa of nitrogen. Local ignition of the reaction sample was achieved within 1–2 s using a nickel-chromium filament that was electrically heated to 900–1000 °C. A computer-assisted data logger (GL100A, Graphtec Co., Japan) continuously recorded the temperature–time history of the process at a rate of 10 Hz.

After completion of the combustion, the burnt sample was cooled to room temperature. Its surface layer (1–2 mm) was mechanically removed and the main sample was transferred to a 500 mL beaker for further purification. The reaction by-products were removed by mixing the sample with diluted HCl in a 500 mL glass beaker on a hot magnetic stir plate. The acid-leached powder was rinsed with distilled water and dried at 80–100 °C.

A thermogravimetric analyser **(**TGA/DSC-1, Mettler Toledo, USA) was used to determine the ignition temperature of the initial mixture, the weight loss, and the heat flow rate. The crystal structures and morphology of the final powders were characterized using an X-ray diffractometer with Cu Kα radiation (Siemens D5000, Germany), a field-emission scanning electron microscope (JEOL JSM-6700F), and transmission electron microscope (TEM, JEOL JEM-1400, Japan). Raman scattering spectra were obtained at room temperature using a Horiba Jobin Yvon LABRAM-HR800 laser micro-Raman spectrometer with a 633 nm laser. Fourier transform infrared spectroscopy (FTIR) analysis was performed on a Biorad FTS-175C Fourier transform infrared spectra spectrometer.

Conclusions

In summary, we have demonstrated a facile combustion synthesis route for preparing few-atomic-layer BN sheets from a B_2O_3+(3+0.5k)Mg+kNH_4Cl system for a *k*=5-7 interval (*k* is the mol number of NH_4Cl). Temperature-time profiles recorded by thermocouples indicated the existence of two independent chemical processes. The first process involves the reaction of Mg+2NH_4Cl, which occurs in the initial stage of the combustion process; then, the reduction of B_2O_3 by Mg and the nitridation of reduced boron follows. The XRD patterns, Raman spectra, and FTIR spectra show that the products are pure and have high crystallinity. From HRTEM and FE-SEM images, the synthesized nanosheets of h-BN were found to consist of a 5- to 10-atom layer; the lateral dimensions of individual sheets ranged from 50 to 1000 nm.

Our experimental study demonstrates the ability of the developed method to isolate hexagonal BN nanosheets consisting of just a few atomic layers. The synthesis method presented here opens the door to the large scale synthesis of few-atomic-layer h-BN nanosheets in an efficient and cost-effective manner.

Acknowledgements

This work was supported by the Korea Institute of Energy Research (No. B4-2444-03)

Notes and references

[a]*Graduate School of Department of Advanced Materials Engineering, Chungnam National University, 99 Daehak-ro, Yuseong-gu, Daejeon 305-764, Republic of Korea*

[b]*Graduate School of Energy Science and Technology, Chungnam National University, 99 Daehak-ro, Yuseong-gu, Daejeon 305-764, Republic of Korea*

[c]*RASOM, Chungnam National University, 79 Daehak-ro, Yuseong-gu, Daejeon 305-764, Republic of Korea*

[d]*Energy Materials Center, Korea Institute of Energy Research, 152 Gajeong-ro, Yuseong-gu, Daejeon 305-343, Republic of Korea*

Electronic Supplementary Information (ESI) available: Thermochemical analysis; Photoluminescence spectra; FE-SEM images..

1. Y. Kubota, K. Watanabe, O. Tsuda, T. Taniguchi, *Science* 2007, **317**, 932.
2. T. Sugino, T. Tai, *Jpn. J. Appl Phys., Part 2* 2000, **39**, L1101.
3. L. Ci, L. Song, C. Jin, D. Jariwala, D. Wu, Y. Li, A. Srivastava, Z.F. Wang, K. Storr, L. Balicas, F. Liu, et al., *Nat. Mater.,* 2010, **9**, 430.
4. L. Song, L. Ci, H. Lu, P.B. Sorokin, C. Jin, J. Ni, A.G. Kvashnin, D.G. Kvashnin, J.Lou, B.I. Yakobson, et al., *Nano Lett.*,2010, **10**, 3209.
5. Y. Chen, J. Zou, S.J. Campbell, G. Le Caer, *Appl. Phys. Lett.,* 2004, **84**, 2430.
6. K. Watanabe, T. Taniguchi, H. Kanda, *Nat. Mater.*,2004, **3**, 404.
7. A.H. Castro Neto, N.M.R. Peres, K.S. Novoselov, A.K. Geim, *Rev. Mod. Phys.,* 2009, **81**, 109.
8. C.R. Dean, A.F. Young, I. Meric, C. Lee, L. Wang, S. Sorgenfrei, K. Watanabe, T. Taniguchi, P. Kim, K.L. Shepard, et al., *Nat. Nanotechnol.,* 2010, **5**, 722.
9. K. H. Lee, H.J. Shin, J. Lee, I.Y. Lee, G.H. Kim, J.Y. Choi, S.W. Kim, *Nano Lett.,* 2012, **12**, 714.
10. L. Britnell, R.V. Gorbachev, R. Jalil, B.D. Belle, F. Schedin, A. Mishchenko, T. Georgiou, M.I. Katsnelson, L. Eaves, S.V. Morozov, *Science*, 2012, **335**, 947.
11. L. Britnell, R.V. Gorbachev, R. Jalil, B.D. Belle, F. Schedin, M.I. Katsnelson, L. Eaves, S.V. Morozov, A.S. Mayorov, N.M.R. Peres, et al., *Nano Lett,*. 2012, **12**, 1707.
12. K.S. Novoselov, D. Jiang, F. Schedin, T.J. Booth, V.V. Khotkevich, S.V. Morozov, A.K. Geim, *Proc. Natl. Acad. Sci. U.S.A.*, 2005, **102**, 10451.
13. D. Pacilé, J.C. Meyer, C.O. Girit, A. Zettl, *Appl. Phys. Lett.* 2008, **92,** 133107.
14. R.V. Gorbachev, I. Riaz, R.R. Nair, R. Jalil, L. Britnell, B.D. Belle, E.W. Hill, K.S. Novoselov, K. Watanabe, T. Taniguchi, et al., *Small,* 2011, **7**, 465.
15. J.N. Coleman, M. Lotya, A. O'Neill, S.D. Bergin, P.J. King, U. Khan, K. Young, A. Gaucher, S. De, R.J. Smith, I.V. Shvets, et al., *Science,* 2011, **331**, 568.
16. Y. Shi, C. Hamsen, X. Jia, K.K. Kim, A. Reina, M. Hofmann, A.L. Hsu, K. Zhang, H. Li, Z.Y. Juang, et al., *Nano Lett.,* 2010, **10**, 4134.
17. M. Corso, W. Auwarter, M. Muntwiler, A. Tamai, T. Greber, J. Osterwalder, *Science,* 2004, **303**, 217.
18. P. Sutter, J. Lahiri, P. Albrecht, E. Sutter, *ACS Nano*, 2011, *5*, 7303.
19. W. Auwarter, H.U. Suter, H. Sachdev, T. Greber, T., *Chem. Mater.,* 2004, **16**, 343.
20. K.K. Kim, A. Hsu, X. Jia, S.M. Kim, Y. Shi, M. Hofmann, D. Nezich, *Nano Lett.,* 2012, **12**, 161.
21. S. Joshi, D. Ecija, R. Koitz, M. Iannuzzi, A.P. Seitsonen, J. Hutter, H. Sachdev, S. Vijayaraghavan, F. Bischoff, K. Seufert, et al., *Nano Lett.,* 2012, **12**, 5821.
22. A.B. Preobrajenski, A.S. Vinogradov, M.L. Ng, E. Cavar, R. Westerstrom, A. Mikkelsen, E. Lundgren, N. Martensson, *Phys. Rev.,* B 2007, **75,** 245412.
23. A. Ismach, H. Chou, D.A. Ferrer, Y.P. Wu, S. McDonnell, H.C. Floresca, A. Covacevich, C. Pope, R. Piner, M.J. Kim, et al., *ACS Nano*, 2012, **6**, 6378.
24. Y. Gao, W. Ren, T. Ma, Z. Liu, Y. Zhang, W.B. Liu, L.P. Ma, X.

Ma, H.M. Cheng, *ACS Nano,* 2013, **7**, 5199.
25. Y.H. Lee, K. K. Liu, A. Y. Lu, C. Y. Wu, C. T. Lin, W. Zhang, C. Y. Su, C. L. Hsu, T. W. Lin, K. H. Wei, Y. Shi and L. J. Li, *RSC Adv.*, 2012, **2**, 111-115.
26. S. K. Kim, H. Cho, M. J. Kim, H. J. Lee, J. H. Park, Y. B. Lee, H. C. Kim, C. W. Yoon, S. W. Nam and S. O. Kang, *J. Mater. Chem. A*, 2013, **1**, 1976-1981.
27. M. Xu, D. Fujita, H. Chen and N. Hanagata, *Nanoscale*, 2011, **3**, 2 854-2858.
28. X. Wang, C. Zhi , L. Li , H. Zeng, C. Li , M. Mitome, D. Golberg and Y. Bando, *Adv. Mater.*, 2011, **23**, 4072-4076.
29. Z. Zhao, Z. Yang, Y. Wen and Y. Wang, J. Am. Ceram. Soc., *2011*, **94**, 4496–4501.
30. Y. Lin, T.V. Williams, J.W. Connell, *J. Phys. Chem. Lett.,* 2009, **1**, 277.
31. R. Nemanich, S. Solin, and R. Martin, *Phys. Rev. B*, 1981, **23**, 6348
32. Y. Kubota, K. Watanabe, O. Tsuda, T. Taniguchi, *Science,* 2007, **317,** 932.
33. C. Zhi, Y. Bando, C. Tang, D. Golberg, R. Xie, and T. Sekigushi, *Appl. Phys. Lett.,* 2005, **86**, 213110.
34. R. Gao, L. Yin, C. Wang, Y. Qi, N. Lun, L. Zhang, Y. Liu, L. Kang, and X. Wang, *J. Phys. Chem. C.*, 2009, **113** 15160–5.
35. S. Xu, Y. Fan, J. Luo, L. Zhang, W. Wang, B. Yao, and L. An, *Appl. Phys. Lett.,* 2007, **90**, 013115.

